Generating electricity by moving a droplet of ionic liquid along graphene

Jun Yin, Xuemei Li, Jin Yu, Zhuhua Zhang, Jianxin Zhou and Wanlin Guo*

Since the early nineteenth century, it has been known that an electric potential can be generated by driving an ionic liquid through fine channels or holes under a pressure gradient. More recently, it has been reported that carbon nanotubes can generate a voltage when immersed in flowing liquids, but the exact origin of these observations is unclear, and generating electricity without a pressure gradient remains a challenge. Here, we show that a voltage of a few millivolts can be produced by moving a droplet of sea water or ionic solution over a strip of monolayer graphene under ambient conditions. Through experiments and density functional theory calculations, we find that a pseudocapacitor is formed at the droplet/graphene interface, which is driven forward by the moving droplet, charging and discharging at the front and rear of the droplet. This gives rise to an electric potential that is proportional to the velocity and number of droplets. The potential is also found to be dependent on the concentration and ionic species of the droplet, and decreases sharply with an increasing number of graphene layers. We illustrate the potential of this electrokinetic phenomenon by using it to create a handwriting sensor and an energy-harvesting device.

Flow sensors and devices that can collect electricity from flowing water are important in a variety of fields, including the harvesting of electric power, the characterization of electrochemical properties, and real-time medical diagnostics[1–4]. These devices rely principally on streaming potential, an electrokinetic phenomenon in which an electric potential is generated when an electrolyte is driven through narrow pores or gaps by a pressure gradient, but they are limited to specific cases[1]. In 2001 it was theoretically proposed that carbon nanotubes in flowing liquids could generate an electric current[5], and since then there have been a number of experimental demonstrations of such effects[2–4]. However, there are significant discrepancies in the reported results, and competing explanations for the observed effects have been proposed[2–8].

Although graphene is extremely sensitive to external stimulations and adsorptions[9–12], we recently showed that immersed graphene cannot generate a voltage from a flowing liquid[13,14]. This result was subsequently confirmed by work[15] in which graphene transistors were constructed to detect the streaming potential, and no fluid-flow-induced electrical currents were observed in the graphene. These results are in agreement with the classical electrokinetic theory for streaming potential: that is, a potential cannot be induced by a flowing liquid without a pressure gradient. Coulomb drag, a process in which repulsive interactions between electrons in spatially separated conductors allow a current flowing in one of the conductors to induce a voltage drop in the other[16], is also of particular interest in layered or two-dimensional systems such as graphene[17–19]. However, in graphene/liquid systems, electrokinetic phenomena (rather than Coulomb drag) should occur, because an electrical double layer will form at the interface of ionic liquids and graphene. In this Article, we show that a voltage on the order of a few millivolts can be induced by moving a droplet of ionic solution along a strip of graphene. We refer to this effect as a drawing potential. The drawing potential is generated by moving a unique pseudocapacitor formed at the interface of the droplet and graphene along the strip. The drawing potential is proportional to the velocity of the droplet in all the tested salt, acid and alkali solutions.

Drawing potential in graphene

Our monolayer graphene samples were grown on electrochemical polished copper foil by low-pressure chemical vapour deposition[20,21], and the high quality of the samples was identified by Raman characterization (Supplementary Fig. 1). Graphene strips with dimensions of $\sim5 \times 110$ mm^2 were then transferred onto a polyester terephthalate (PET) substrate with unavoidable folded regions by a poly(methyl methacrylate) (PMMA) mediated method[22]. Multilayer graphene samples were obtained by superposing the monolayer graphene, without an organic contamination trapped interlayer, using an improved stacking method (see Methods). Two terminals of the graphene strip were connected with metal wires using silver epoxy to form an ohmic contact (Supplementary Fig. 2).

The experimental set-up is presented in Fig. 1. A droplet of 0.6 M NaCl aqueous solution (simulated sea water) was sandwiched between the graphene surface and a 5×5 mm^2 SiO$_2$/Si wafer, which was placed 1 mm above the graphene surface and was able to move along a track at fixed separation. The liquid droplet could be drawn by the SiO$_2$/Si wafer to move on the graphene surface facilely with advancing and receding contact angles (θ_A and θ_R) of $\sim91.9°$ and $\sim60.2°$, respectively (Fig. 1, inset). The velocity and direction of movement on the wafer were controlled by a variable-speed motor. The area outside the graphene strip was coated with a thin hydrophobic layer of wax to confine the droplet on the graphene strip. The voltage signal was recorded in real time by a Keithley 2010 multimeter, with its positive terminal connected to the right end of the strips.

A typical voltage response to the movement of a droplet on the graphene strip is shown in Fig. 2a. When a droplet (43 µl in volume, unless indicated otherwise) of 0.6 M NaCl solution is

---

State Key Laboratory of Mechanics and Control of Mechanical Structures, Key Laboratory for Intelligent Nano Materials and Devices of the Ministry of Education, and Institute of Nanoscience, Nanjing University of Aeronautics and Astronautics, 29 Yudao Street, Nanjing 210016, China.
*e-mail: wlguo@nuaa.edu.cn

1
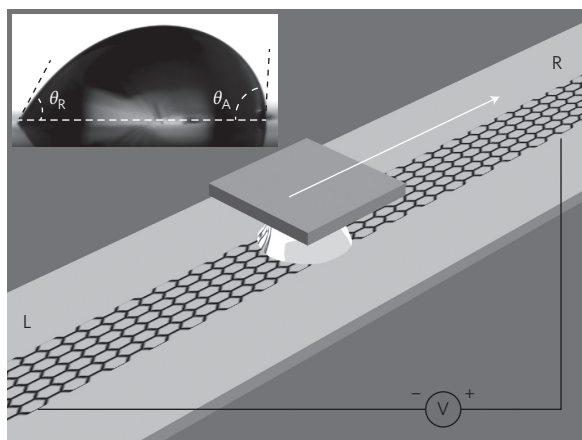
Figure 1 | Illustration of the experimental set-up. A liquid droplet is sandwiched between graphene and a SiO$_2$/Si wafer, and drawn by the wafer at specific velocities. Inset: a droplet of 0.6 M NaCl solution on a graphene surface with advancing and receding contact angles of ~91.9° and ~60.2°, respectively.

drawn from the left to right end of the strip at a constant velocity of 2.25 cm s^{-1}, a voltage of ~0.15 mV is produced. The slight delay in the voltage response to the movement of the droplet is attributed to contact angle hysteresis. When the droplet stops, the voltage drops

sharply to zero. When the droplet moves back from right to left at the same velocity, the induced voltage has the same magnitude, but with reversed sign. The distinguishable step in the induced voltage at constant velocity should reflect the changing properties or quality of the graphene sample along the strip length, while the slight fluctuation of the induced voltage can be attributed to fluctuations in droplet movement.

The induced voltage increases linearly with increasing velocity of the droplet (Fig. 2b) in our testing range. For one droplet of 0.6 M NaCl solution, the induced voltage increases from 0.09 mV at 1.3 cm s^{-1} to 0.59 mV at 8.55 cm s^{-1} and can be fitted perfectly to $V = Av$, with a slope of $A = 6.9$ mV s m^{-1}. It is interesting that the voltage can be multiplied by drawing multiple droplets simultaneously. The induced voltage is in exact proportion to the number of droplets of the same size, and still increases linearly with the moving velocity. The fitting slope A is nearly two and three times that of a single droplet for two and three droplets, respectively. When two droplets on a single graphene sheet are moving in opposite directions, the voltage generated by each individual droplet would offset the other (Supplementary Fig. 3). However, the dependence of the induced voltage on the ion concentration of the solution is not monotonic (Supplementary Fig. 4). We have also shown that the magnitude of the induced voltage can be enlarged by increasing the size of the droplet (Supplementary Fig. 5).

Based on the robust linear relationship between the voltage and velocity, graphene can be used to sense the velocity of a moving
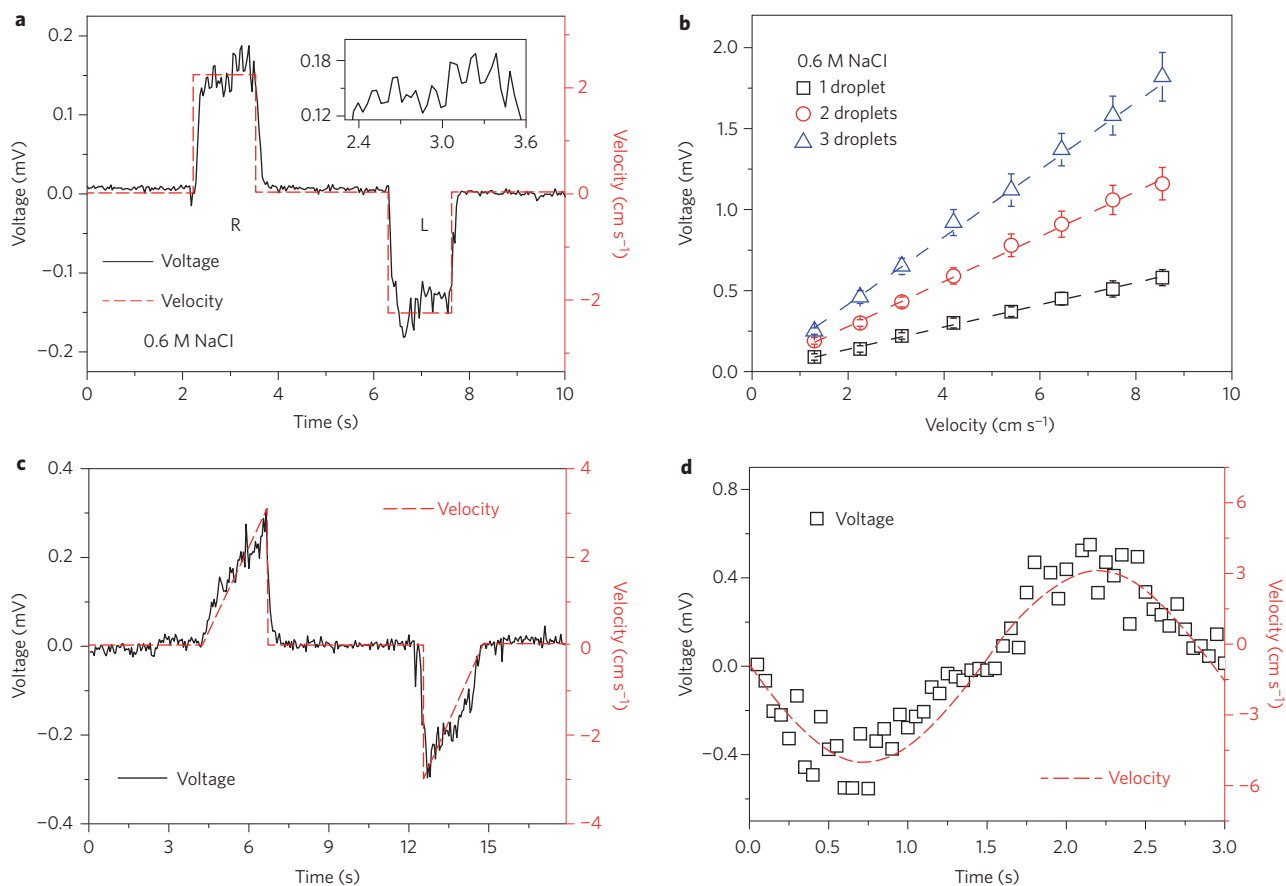
Figure 2 | Voltage induced in graphene by drawing one or more droplets of 0.6 M NaCl solution. a, Typical voltage signal produced by drawing a droplet on a graphene strip from left (L) to right (R) ends and then back. The inset highlights the voltage signal during the movement of the droplet. **b,** Voltage induced by moving one, two and three droplets. Dashed lines are curves linearly fitted to the measured data. The error bars represent the amplitudes of fluctuation in the voltage signal as highlighted by the inset in **a**. **c,d,** Voltage response to triangular-wave-like (**c**) and sine-wave-like (**d**) velocity of movement (red dashed lines) of a droplet.
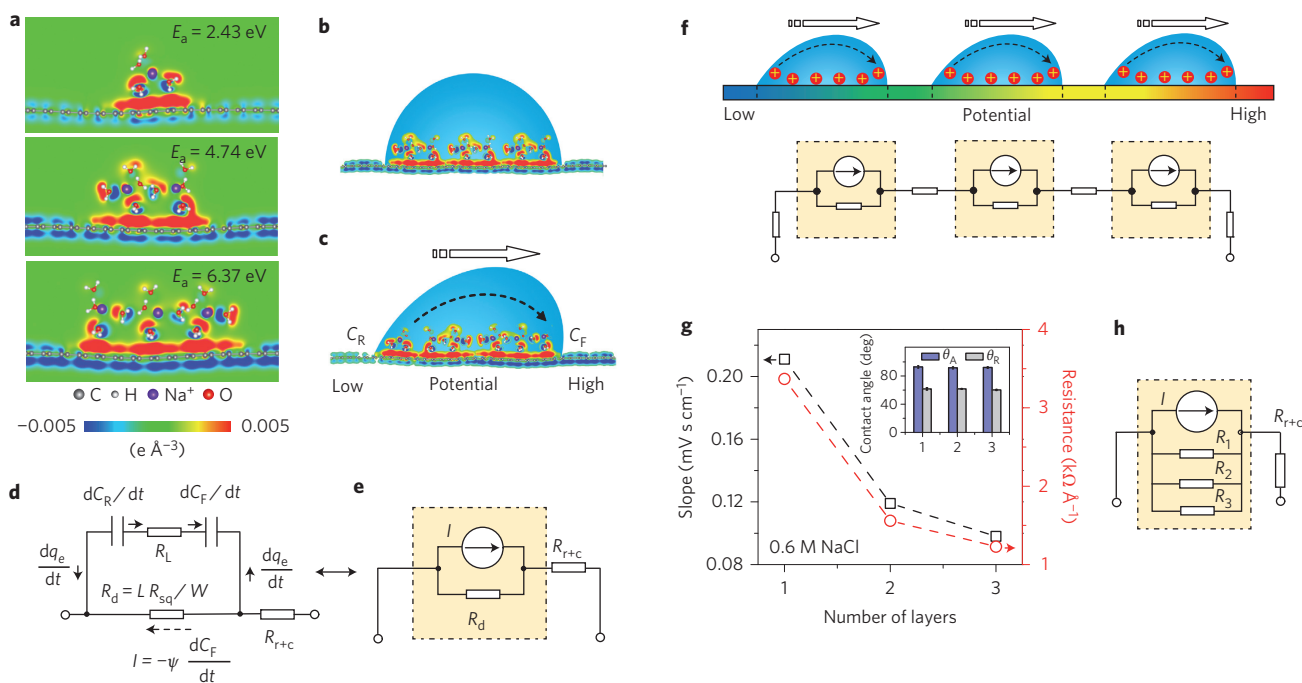
Figure 3 | Mechanism for the drawing potential. a, DFT results for the distribution of differential charge near monolayer graphene caused by adsorbing one to three rows of hydrated sodium cations, and the corresponding adsorption energy (E_a). **b,** Schematic illustration of the pseudocapacitance formed by a static droplet on graphene. **c,** Schematic illustration of the potential difference induced by a moving droplet. **d,** Equivalent circuit for **c**. Solid arrows indicate the flow direction of electrons in graphene and Na$^+$ ions in the droplet. **e,** Simplified circuit of the system. **f,** Schematic illustration and equivalent circuit for three moving droplets on graphene. **g,** Drawing potential and resistance change with number of graphene layers. Inset: Advancing and receding contact angles of the solution on single-, bi- and trilayer graphene. **h,** Equivalent circuit for a moving droplet on trilayer graphene.

droplet on it. Figure 2c shows that the induced voltage can excellently reflect the triangular-wave-like velocity (dashed lines) of a droplet of 0.6 M NaCl on graphene. When the droplet moves sinusoidally in terms of velocity, a sine-wave-like voltage response can be detected (Fig. 2d).

Mechanism

According to classic electrokinetic theory, when a solid surface is in touch with an ionic solution, a layer of ions, either cations or anions, will adsorb to the surface due to an electrochemical interaction, and a second layer comprising counter-ions will be attracted to the first layer via the Coulomb force, thereby forming an electrical double layer[23]. Simultaneously, reversible Faradaic charge transfer occurs near the solid surface at the adsorbed first layer of ions, leading to pseudocapacitance at the liquid–solid interface. Specific to the graphene in contact with a NaCl aqueous solution, our density functional theory (DFT) calculations show that a hydrated Na$^+$ ion can be adsorbed on the graphene with an adsorption energy of over 2 eV (Fig. 3a), while a hydrated Cl$^-$ anion is repulsive to graphene because of its negative adsorption energy[13]. The ionic adsorption is physisorption, as the surrounding water molecules can impede the direct interaction between the graphene and ions. Our DFT calculations show that the adsorbed hydrated sodium cations draw image electrons from the graphene, causing significant electron accumulation on the upper surface of the graphene, as shown by the distribution of differential charge in Fig. 3a. With increasing number of adsorbed hydrated Na$^+$, a thin electron accumulation layer extends along the upper surface of the graphene, forming a pseudocapacitor with the adsorbed Na$^+$ layer. As the interlayer distance between the positive hydrated Na$^+$ layer and the negative electron layer is only ~0.4 nm, the formed pseudocapacitance is remarkable. The accumulation of electrons on the upper surface of the graphene drawn by the adsorbed sodium cation layer leads to

depletion of electrons at the other side of the graphene and around the cation-covered region.

For a static NaCl droplet on graphene, the charge redistributes symmetrically on both sides of the droplet on the graphene, and there is no potential difference between its left and right sides (Fig. 3b). When the droplet is drawn into moving on the graphene, ions are adsorbed at the front end, advancing the pseudocapacitor forward and drawing electrons in the graphene. Meanwhile, ions are being desorbed at the rear of the droplet, discharging the pseudocapacitor and releasing the electrons to the graphene. This entire process gives rise to an increase/decrease in electron density behind/ahead of the moving droplet (as illustrated schematically in Fig. 3c) compared to the static state, resulting in a higher potential at the front than at the rear.

Considering the dynamic front and rear boundaries of the droplet as capacitors C_F and C_R in charging and discharging modes, respectively, the dynamical process can be described by the equivalent electrical circuit in Fig. 3d, where R_L, R_d and R_{r+c} represent the resistances across the liquid, the graphene under the droplet, and the graphene outside the droplet combined with the contact resistance, respectively. The charging of C_F and simultaneous discharging of C_R drive the free electron moving from the rear to the front end, across the graphene under the droplet. Taking the pseudocapacitance per unit area, C_0, to be determined by the graphene–solution system, the changing rates of the pseudocapacitance at the front and rear can be calculated as $dC_F/dt = C_0 W v$ and $dC_R/dt = -C_0 W v$ for a droplet moving at velocity v from left to right, where W is the width of the graphene strip under the droplet. An equivalent current across the graphene section under the droplet can then be evaluated from the rate of transferred electrons dq_e/dt as

$$I = -\frac{dq_e}{dt} = \psi \frac{dC_F}{dt} = -\psi \frac{dC_R}{dt} = -\psi W C_0 v \qquad (1)$$

where ψ is defined as the equivalent surface potential of graphene relative to the adsorbed hydrated Na^+ layer. Then, the induced open-circuit voltage is given by

$$V = R_d I = -LR_{sq}\psi C_0 V \qquad (2)$$

where R_{sq} is the square resistance of the graphene and L is the length of the droplet. For convenience, the equivalent circuit for voltage generation in the system can be further simplified to a current source I with an internal resistance R_d, as shown in Fig. 3e. Consistent with the model, the developed voltage is proportional to the velocity of the droplet with a slope of $A = -LR_{sq}\psi C_0$ and can be enlarged by a droplet with larger volume, which increases the contact length L. For the narrow gap between the positive and negative charged layers, C_0 should be exceptionally high. This can explain why drawing a tiny droplet on graphene can produce voltage up to millivolt order. According to the proposed model, the multiplying of the induced voltage by an array of droplets can be considered as a series connection of multiple current sources with internal resistances, as shown in Fig. 3f.

To further check the proposed mechanism and the equivalent circuit, we conducted an experiment on few-layer graphene strips. Because the few-layer graphene shows the same advancing and receding contact angles as the monolayer graphene (Fig. 3g, inset), it is reasonable to assume that the contact area to a droplet of the same volume and the formed pseudocapacitance remain unchanged. Therefore, according to the model, the induced voltage should be proportionally reduced by the decrease in sheet resistance. It is shown that the slopes of the voltage–velocity curves for the mono-, bi- and trilayer graphene samples decrease in proportion to the square resistance of the samples (Fig. 3g). Additional graphene layers provide additional channels for electron flow back from the rear to the front, reducing the drawing potential in the graphene, as shown in Fig. 3h. This strong layer-dependence of the drawing potential supports the proposed mechanism and equivalent circuit well. Although it is possible that other conductive and semiconductor materials may show similar voltages when an ionic liquid droplet passes over them (in accordance with the mechanism), we have not been able to find a candidate material that can satisfy the strict requirements for this, including suitable wettability and resistance, stability under ambient conditions, and sufficiently thin to eliminate possible channels for the circumfluence of charge.

As is expected from the electric double-layer theory, the drawing potential should depend on the ion species. We therefore conducted further experiments using aqueous solutions of different salts, acid and alkali. Although the advancing and receding contact angles of the liquids on the graphene remain nearly unaffected by ion species (except for HCl solution, Fig. 4a), the drawing potential in the graphene shows a strong dependence on ion species (Fig. 4b). Compared with the case of NaCl, the drawing potential shows large differences in magnitude, and even in sign. No detectable drawing potential for deionized water can be found, even at velocities up to 8.55 cm s^{-1} (Supplementary Fig. 6), as nearly no ion presents to form the pseudocapacitance. The voltage induced by three droplets of $NH_3 \cdot H_2O$ and $MgCl_2$ is ~2.6 and ~1.5 times that induced by the same number of NaCl droplets, suggesting that these droplets can draw larger amounts of image electrons. The sign of the voltage induced by droplets of HCl solution is reversed. We have previously shown that hydronium H_3O^+ ions in HCl solution can absorb much more strongly on a graphene surface[13]. This exceptionally high adsorption energy is also considered to be the reason for the smaller advancing and receding contact angles of HCl solution on graphene compared with other ionic solutions. Once wetted by HCl solution, the graphene surface would absorb a layer of H_3O^+ to behave like a positively charged sheet, which attracts Cl^- anions. So the dynamic
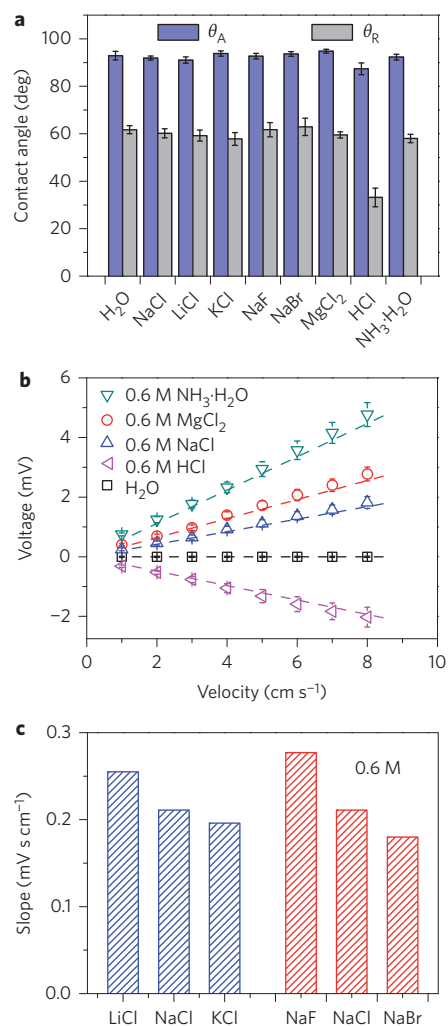
**Figure 4 | Contact angles and drawing potential for various ionic solutions on monolayer graphene. a**, Advancing and receding contact angles of deionized water and different 0.6 M solutions on graphene. **b**, Voltage induced by three droplets of different solutions. **c**, Fitted slope $A = V/v$ for three droplets of different chloride and sodium salts.

pseudocapacitance should be dominated by the Cl^-, resulting in a voltage with reversed direction. The strong adsorption of the H_3O^+ on graphene, even after removing the droplet, can be proven by the reduced water contact angle on graphene that has been wetted by HCl solution, even after rinsing with deionized water for 30 min (Supplementary Fig. 7).

The voltage slopes induced by drawing droplets of solutions of chloride salts with different alkali metal cations and sodium salts with different halide anions are compared in Fig. 4c. It is interesting that the induced voltage decreases with increasing atomic number for both the cations in chloride salts and anions in sodium salts. We attribute this to the different abilities of alkali metal cations to draw electrons from graphene and the weaker screening effect induced by F^- compared to Cl^- and Br^-, despite the fact that they have the same concentration.

Demonstration of applications

To demonstrate possible applications of the drawing potential, we used a square graphene sheet to sense handwriting using a Chinese brush dipped in 0.01 M NaCl solution. Two pairs of electrodes, E1$^+$–E1$^-$ (right–left) and E2$^+$–E2$^-$ (bottom–top), were patterned perpendicularly on the four sides of the graphene to
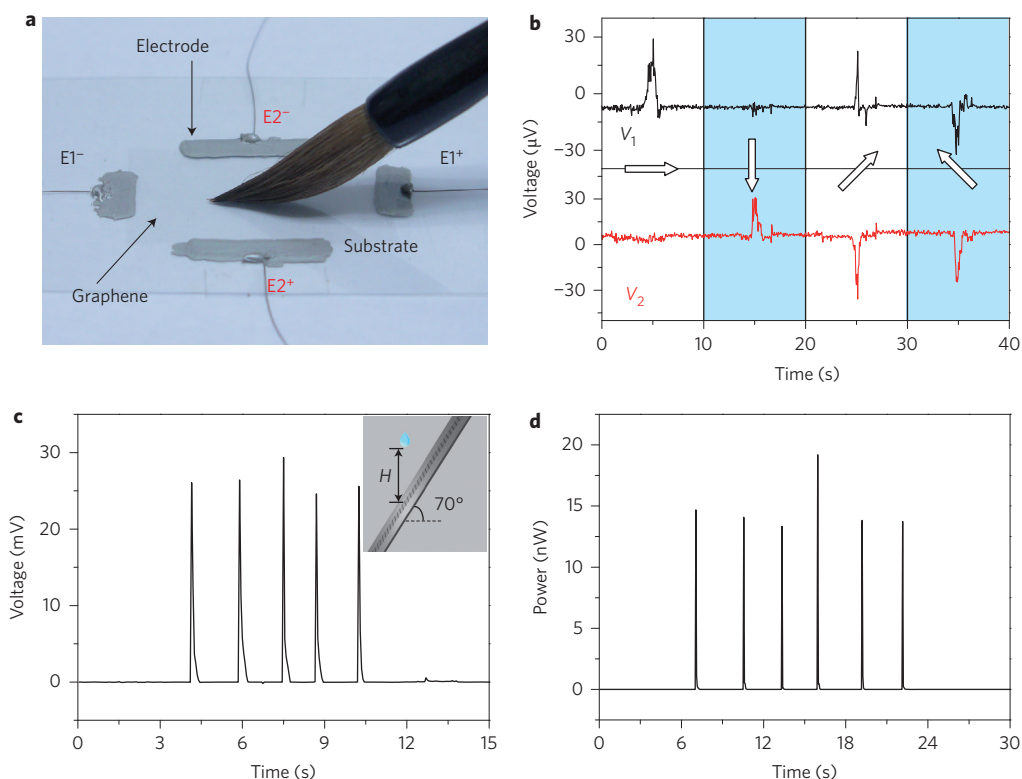
Figure 5 | Applications of the drawing potential. a, Photograph of handwriting with a Chinese brush on graphene. **b**, Sensing the stroke directions (arrows) by the drawing potentials between electrodes E1+– E1− and E2+– E2− as shown in **a**. **c,d**, Voltage (**c**) and power (**d**) produced by dropping droplets of 0.6 M CuCl$_2$ solution onto graphene at an angle of 70° (inset) from a height of 15 cm. The output power is measured through a connected load $R = 17.4$ kΩ.

distinguish the handwriting direction (Fig. 5a). The voltage induced between the electrodes shows different characteristics for different drawing directions, as shown in Fig. 5b. The induced voltage V_1 between E1+ and E1− can sense the horizontal component as positive for left-to-right drawing, while voltage V_2 between E2+ and E2− senses the vertical component as positive for top-to-down drawing. For example, a drawing from bottom left to top right produces positive V_1 and negative V_2, and so on. Based on the detected voltage, the basic strokes written on the graphene surface can be recognized easily. Furthermore, the magnitudes of the induced voltages also contain rich information, yet to be explored, about the sharpness of the pen tip and the force and speed of the handwriting. The microvolt order of the handwriting-induced voltage is mainly due to the large size of the graphene in comparison to the width of the strokes, as the graphene outside the drawing path serves as an additional channel to release the drawing potential, similar to the function of additional graphene layers. Compared to arrays of conductivity sensors that need a power supply, the prototype shows notable advantages in terms of its simple structure and energy-harvesting character.

Finally, a prototype of an energy-harvesting device was demonstrated. As shown in Fig. 5c, dropping a droplet of 80 μl 0.6 M CuCl$_2$ solution onto a 70° tilted graphene surface from 15 cm above the contact point under gravity can generate a pulse voltage of ∼30 mV, with a corresponding short-circuit current of ∼1.7 μA. Connecting a load of 17.4 kΩ, the measured output power can reach 19.2 nW with a corresponding efficiency of ∼1% (Supplementary Section 2), as shown in Fig. 5d. This enhanced voltage and output power can be attributed to the larger velocity of the droplet as well as the greater droplet size when crashed onto the tilted graphene surface. In practice, many alternative ways can also be adopted for this energy harvesting, such as a droplet flowing in the valley of folded paper.

Conclusions

We have reported a drawing potential effect in graphene. Droplets of ionic liquids moving on graphene can generate electricity due to a novel electrokinetic phenomenon in which a pseudocapacitor formed under the droplet is driven forward, charging and discharging at the boundary of the droplet. This mechanism allows the creation of various prototypes, including a velocity sensor, a handwriting sensor and an energy-harvesting device.

Methods

by 20 Å along the normal direction (Supplementary Fig. 8). Dipole correction[29] was considered to exclude the artificial dipole–dipole interaction between adjacent images in repeated units. The geometry was fully relaxed without any constraint by using the conjugate gradient method until the force on each atom was less than 0.01 eV Å^{-1}. The adsorption energy for hydrated ions adsorbed on graphene was calculated using $E_a = E_g + E_{hi} - E_{system}$, where E_g, E_{hi} and E_{system} are the energies of graphene, a hydrated ion and the combined system of them, respectively.

References

1. Delgadoa, A. V. *et al.* Measurement and interpretation of electrokinetic phenomena. *J. Colloid Interface Sci.* **309,** 194–224 (2007).
2. Ghosh, S., Sood, A. K. & Kumar, N. Carbon nanotube flow sensors. *Science* **299,** 1042–1044 (2003).
3. Zhao Y. *et al.* Individual water-filled single-walled carbon nanotubes as hydroelectric power converters. *Adv. Mater.* **20,** 1772–1776 (2008).
4. Liu, J., Dai, L. & Baur, J. W. Multiwalled carbon nanotubes for flow-induced voltage generation. *J. Appl. Phys.* **101,** 064312 (2007).
5. Král, P. & Shapiro, M. Nanotube electron drag in flowing liquids. *Phys. Rev. Lett.* **86,** 131–134 (2001).
6. Yuan, Q. & Zhao, Y. P. Hydroelectric voltage generation based on water-filled single-walled carbon nanotubes. *J. Am. Chem. Soc.* **131,** 6374–6376 (2009).
7. Persson, B. N., Tartaglino, J. U., Tosatti, E. & Ueba, H. Electronic friction and liquid-flow-induced voltage in nanotubes. *Phys. Rev. B* **69,** 235410 (2004).
8. Cohen, A. E. Carbon nanotubes provide a charge. *Science* **300,** 1235–1236 (2003).
9. Schedin, F. *et al.* Detection of individual gas molecules adsorbed on graphene. *Nature Mater.* **6,** 652–655 (2007).
10. Robinson, J. T., Perkins, F. K., Snow, E. S., Wei, Z. & Sheehan, P. E. Reduced graphene oxide molecular sensors. *Nano Lett.* **8,** 3137–3140 (2008).
11. Wehling, T. O. *et al.* Molecular doping of graphene. *Nano Lett.* **8,** 173–177 (2008).
12. Fowler, J. D. *et al.* Practical chemical sensors from chemically derived graphene. *ACS Nano* **3,** 301–306 (2009).
13. Yin, J., Zhang, Z. H., Li, X. M., Zhou, J. X. & Guo, W. L. Harvesting energy from water flow over graphene? *Nano Lett.* **12,** 1736–1741 (2012).
14. Dhiman, P. *et al.* Harvesting energy from water flow over graphene. *Nano Lett.* **11,** 3123–3127 (2011).
15. Newaz, A. K. M., Markov, D. A., Prasai, D. & Bolotin, K. I. Graphene transistor as a probe for streaming potential. *Nano Lett.* **12,** 2931–2935 (2012).
16. Nandi, D., Finck, A. D. K., Eisenstein, J. P., Pfeiffer, L. N. & West, K. W. Exciton condensation and perfect Coulomb drag. *Nature* **488,** 481–484 (2012).
17. Gorbachev, R. V. *et al.* Strong Coulomb drag and broken symmetry in double-layer graphene. *Nature Phys.* **8,** 896–901 (2012).
18. Weber, C. P. *et al.* Observation of spin Coulomb drag in a two-dimensional electron gas. *Nature* **437,** 1330–1333 (2005).
19. Price, A. S., Savchenko, A. K., Narozhny, B. N., Allison, G. & Ritchie, D. A. Giant fluctuations of coulomb drag in a bilayer system. *Science* **316,** 99–102 (2007).
20. Yan, Z. *et al.* Toward the synthesis of wafer-scale single-crystal graphene on copper foils. *ACS Nano* **6,** 9110–9118 (2012).
21. Li, X. *et al.* Large-area synthesis of high-quality and uniform graphene films on copper foils. *Science* **324,** 1312–1314 (2009).
22. Li, X. *et al.* Transfer of large-area graphene films for high-performance transparent conductive electrodes. *Nano Lett.* **9,** 4359–4363 (2009).
23. Lyklema, J. J., de Keizer, A., Bijsterbosch, B. H., Fleer, G. J. & Cohen Stuart, M. A. *Fundamentals of Interface and Colloid Science* (Academic, 1995).
24. Kresse, G. & Furthmuller, J. Efficient iterative schemes for *ab initio* total-energy calculations using a plane-wave basis set. *Phys. Rev. B* **54,** 11169–11186 (1996).
25. Kresse, G. & Furthmuller, J. Efficiency of *ab-initio* total energy calculations for metals and semiconductors using a plane-wave basis set. *Comput. Mater. Sci.* **6,** 15–50 (1996).
26. Perdew, J. P., Burke, K. & Ernzerhof, M. Generalized gradient approximation made simple. *Phys. Rev. Lett.* **77,** 3865–3868 (1996).
27. Kresse, G. & Joubert, D. From ultrasoft pseudopotentials to the projector augmented-wave method. *Phys. Rev. B* **59,** 1758–1775 (1999).
28. Kielland, J. Chemical hydration numbers. *J. Chem. Educ.* **14,** 412–413 (1937).
29. Makov, G. & Payne, M. C. Periodic boundary conditions in *ab initio* calculations. *Phys. Rev. B* **51,** 4014–4022 (1995).

Acknowledgements

Author contributions

W.G. conceived the project and designed the experiments with J.Yin. J.Yin, X.L. and J.Z. performed the experiments. J.Yu and Z.Z. performed the calculations. W.G., J.Yin and J.Yu analysed the data. W.G., J.Yin and Z.Z. wrote the paper. All authors discussed the results and commented on the manuscript.

Additional information

Supplementary information is available in the online version of the paper. Reprints and permissions information is available online at www.nature.com/reprints. Correspondence and requests for materials should be addressed to W.G.

Competing financial interests

The authors declare no competing financial interests.